

# Loss Locational Sensitivity in Distribution Systems

Abdullah Alburidy  
Electrical Engineering Department  
University of South Florida, Tampa, USA  
Qassim University, Saudi Arabia  
alburidy@mail.usf.edu

Lingling Fan, *Senior Member, IEEE*  
Smart Grid Power Systems Laboratory  
Electrical Engineering Department  
University of South Florida, Tampa, USA  
linglingfan@usf.edu

**Abstract**—This paper demonstrates the use of dual variables associated with power equality constraints in Volt/VAR optimization models as a loss locational sensitivity. The dual variables can be employed for optimal placement of VAR compensation equipment and distributed energy resources (DERs). In addition, it can be utilized to price DERs generated power. The concept is illustrated thoroughly and tested on a modified IEEE-69 bus distribution system and results are presented and discussed. A comprehensive nonlinear programming formulation of distribution system Volt/VAR optimization model is illustrated. Furthermore, a penalty-based approach that handle discrete or integer variables and solve MINLP as continuous NLP is reviewed and validated. The presented formulation is able to directly allocate the dual variables values.

**Index Terms**—Loss factor, locational Sensitivity, locational marginal price, LMP, Distribution Systems, DERs, VVO, MINLP, VOLT/VAR optimization.

## I. INTRODUCTION

Loss locational sensitivity (i.e. loss factor) is an essential part of power system analysis as it evaluates the reaction of power loss at a certain location of the system to power injection or withdrawal. With the recent advancement of power computational tools and integration of distributed energy resources (DERs), inspecting loss sensitivity in distribution network has gained more attention and become a subject of interest to elect optimal placement of volt/VAR equipment or to optimize active or reactive power levels. [1]–[3].

VAR compensation equipment such as shunt capacitor banks, static VAR compensators (SVCs) and DER inverters with reactive power support capabilities improves the system voltage profile, helps to diminish voltage fluctuation and reduces power losses. This yields further power reliability, increases loading capacity and lengthens lifespan of equipment. Abundant methods, such as metaheuristic-algorithms and evolutionary-based strategies are employed to specify optimal sizing and allocation to integrate these equipment [4], [5]. The presented concept offers a valid tool to validate those solutions.

Furthermore, as an alternative of setting a flat rate for DERs power supply which might be unreasonable in locations with high demand and low supply, the results of the highlighted concept can be utilized to assign variety of percentage rates based on the location of participants. This will encourage DERs holders in areas with elevated power demand and losses

to participate and supply local demands which will improve the system power equality, lower losses and limit congestion.

In optimal power flow and wholesale energy market optimization models, the objective function essentially aims to minimize power generation costs in addition to other auxiliary functions such as conservation voltage reduction and reducing equipment switching costs. One of the essential constraints in these optimization models is power balance equality. In these models, the objective function revolves around costs and prices. Hence, the dual variables associating power balance equality constraints ( $\lambda_i$ ) are customarily referred to as locational marginal prices (LMPs). Those variables indicate the cost of supplying an additional unit to meet demand at a particular location. However, in Volt/VAR optimization models, the objective function mainly aims to minimize power losses and maintains a proper voltage profile across distribution branches. In this case, the dual variables associated with the power balance equation constraints indicate to the locational sensitivity of loss toward active or reactive load alteration. This paper highlights the potential applications of analyzing these dual variables conducted values and utilizing them as loss factors that measure the sensitivity of loss toward power level variations.

Various literatures are proposing different Volt/Var Optimization (VVO) methodologies and loss sensitivity calculation in distribution network [6], [7]. Cascaded optimization approaches are employed to first allocate network equipment optimal settings and then perform a market clearance problem to calculate the dual variable values. The presented approach in this paper can compute network optimal settings including integer variables in conjunction with the dual variables values simultaneously.

In this paper, a mixed-integer non-linear optimization problem (MINLOP) is adopted to model modern radial distribution systems. The model incorporates on-load tap-changing distribution transformers, step voltage regulators (SVRs), capacitor banks (CBs) and distributed energy resources (DERs). A penalty-based nonlinear approach which can tackle integer variables is employed to rapidly solve the MINLOP model and allocate optimal results with fairly high precision. This approach converts integer variables into continuous ones and implement a penalty function to the objective function to force those variables to take integer values [8], [9]. As a contribution to this approach, discrete variables were expressed

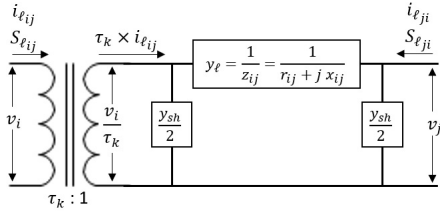


Fig. 1: A unified  $\pi$ -model for distribution branches.

in terms of integer variables and implemented directly into the optimization model producing more divine and logical outcomes.

## II. DISTRIBUTION SYSTEM VOLT/VAR OPTIMIZATION

### A. System Modeling

1) *Radial Distribution Branches, OLTCs and VRs*: A unified  $\pi$ -model as shown in Fig. 1 is adopted to model distribution branches with constant impedance, such as overhead lines and underground cables, as well as branches with controllable impedance for lines with voltage regulators (VRs) and on-load tap-changing transformers (OLTCs).

Fig. 1 depicts a branch  $\ell$  connecting two nodes where  $i$  is the sending node and  $j$  is the receiving node. The parameter  $y_{sh}$  denotes the total charging susceptance at node  $i$  where  $y_{sh} = j b_c$ . The variable  $\tau_k$  is a discrete variable denotes OLTC or voltage regulator (VR) tap regulation-ratio where  $k$  represents the equipment number. It can be expressed as,

$$\tau_k = \tau_k^{\min} + U_{t_k} \times \delta_k^t, \quad U_{t_k} \in \mathbb{Z} \quad (1)$$

where  $\tau_k^{\min}$  is the lower limit of  $\tau_k$  while  $U_{t_k}$  is an integer variable denotes transformer  $k$  OLTC's tap position number while  $\delta_k^t$  represents the OLTC incremental/decremental tap step-size.

As the tap-ratio  $\tau_k$  magnitude varies, the system admittance matrix changes accordingly. Hence, the bus admittance matrix of this branch, which relates current injections to nodal voltages, can be formulated as [10],

$$Y_{\text{bus}} = \begin{bmatrix} (y_{\ell} + j \frac{b_c}{2}) \frac{1}{\tau_k^2} & -y_{\ell} \frac{1}{\tau_k} \\ -y_{\ell} \frac{1}{\tau_k} & y_{\ell} + j \frac{b_c}{2} \end{bmatrix} = \begin{bmatrix} Y_{ii} \frac{1}{\tau_k^2} & Y_{ij} \frac{1}{\tau_k} \\ Y_{ji} \frac{1}{\tau_k} & Y_{jj} \end{bmatrix} \quad (2)$$

When a branch is not equipped with an OLTC or VR, the variable  $\tau_k$  should be set to 1.

For a branch  $\ell$  connecting two nodes  $i$  and  $j$ , the apparent, active and reactive power flow can be computed as,

$$S_{ij}(t) = |V_i|^2 Y_{ii}^* \frac{1}{\tau_k^2} + |V_i||V_j| Y_{ij}^* \frac{1}{\tau_k} (\cos \theta_{ij} + j \sin \theta_{ij}) \quad (3)$$

$$P_{ij}(t) = -G_{ij} |V_i|^2 \frac{1}{\tau_k^2} + |V_i||V_j| \frac{1}{\tau_k} [G_{ij} \cos \theta_{ij} + B_{ij} \sin \theta_{ij}] \quad (4)$$

$$Q_{ij}(t) = B_{ij} |V_i|^2 \frac{1}{\tau_k^2} - |V_i||V_j| \frac{1}{\tau_k} [B_{ij} \cos \theta_{ij} - G_{ij} \sin \theta_{ij}] \quad (5)$$

where  $Y_{ij}^* = G_{ij} - jB_{ij}$  is the  $i$ -th row and  $j$ -th column in the system total admittance matrix.

Active power losses across distribution branch  $\ell$  are calculated as,

$$P_{ij}^{\text{loss}}(t) = \text{Re}(S_{ij} + S_{ji}) = -G_{ij} \left[ |V_i|^2 \frac{1}{\tau_k^2} + |V_j|^2 - 2|V_i||V_j| \frac{1}{\tau_k} \cos \theta_{ij} \right] \quad (6)$$

2) *Shunt Capacitor Banks*: The quantity of reactive power injection relies on the node's voltage magnitude and it can be computed as:

$$Q_k^{\text{sh}} = b_k^{\text{sh}} |V_k|^2 \quad (7)$$

where  $b_k^{\text{sh}}$  is a discrete variable quantifies the shunt susceptance at node  $k$  in pu. It can be expressed as,

$$b_k^{\text{sh}} = b_k^{\min} + U_{c_k} \times \delta_k^c, \quad U_{c_k} \in \mathbb{Z} \quad (8)$$

where  $b_k^{\min}$  is the lower limit of  $b_k^{\text{sh}}$  and  $U_{c_k}$  is an integer variable denotes the capacitor bank  $k$  tap position number. The parameter  $\delta_k^c$  denotes capacitor bank  $k$  incremental/decremental tap step-size.

The amount of VARs injection can be adjusted by varying the tap position variable  $U_{c_k}$ . If node  $k$  is not equipped with a capacitor bank then  $Q_k^{\text{sh}}$  should be set to zero.

3) *Photovoltaic Systems (PV)*: A PV-system with VAR supply capability is chosen here to represent DERs due to its widespread use. When a distributed generation unit such as PV-system is interfaced with a voltage source converter (VSC), it can provides a mechanism to control nodal voltage by injection or absorbing reactive power along with active power. Nevertheless, reactive power support depends on the inverter power capacity. The system priority is to dispatch maximum active power and then depending on the residual capacity of the inverter; reactive power is dispatched (generated or absorbed).

$$Q_{i,g}^{\text{PV}} \leq \sqrt{(S_{\text{rated}}^{\text{PV}})^2 - (P_{i,g}^{\text{PV}})^2} \quad (9)$$

where  $S_{\text{rated}}^{\text{PV}}$  is the inverter apparent power (VA),  $P_{i,g}^{\text{PV}}$  and  $Q_{i,g}^{\text{PV}}$  are the generated active and reactive power respectively. Obviously, at maximum active power generation, the inverter will not be able to provide any reactive power. Hence, it is important to oversize the inverter. A 10% increase in the inverter capacity will rise reactive power support capability at maximum active power generation from 0% to about 46% of its full potential [11].

### B. VVO Model Formulation

Typical VVO model for distribution systems with centralized control unit is a mixed-integer nonlinear problem (MINLP) that aims to minimize active power loss across distribution branches at all time segments while satisfying power operational and security constraints. The decision variables are: on load tap-changer and voltage regulator tap position  $U_{t_k}$ , shunt capacitor banks tap position  $U_{c_k}$ , PV-system inverters VAR supply  $Q_{i,g}^{\text{PV}}$  and nodal voltage magnitude and angle ( $|V_i|, \theta_i$ ). The model is generally formulated as:

$$\min_x \sum_{t=1}^{\mathcal{T}} \sum_{\ell} P_{\ell}^{loss}(t) \cdot [T_{t+1} - T_t] \quad (10a)$$

$$\text{s.t. } \Delta \mathcal{P}_i(t) = 0 \quad \forall i \in \mathcal{N} \quad \forall t \in \mathcal{T} : \lambda_i^P(t) \quad (10b)$$

$$\Delta \mathcal{Q}_i(t) = 0 \quad \forall i \in \mathcal{N} \quad \forall t \in \mathcal{T} : \lambda_i^Q(t) \quad (10c)$$

$$\mathcal{S}_{\ell}(t) \leq \mathcal{S}_{\ell}^{max} \quad \forall \ell \in \mathcal{L} \quad \forall t \in \mathcal{T} : \mathfrak{S}_{\ell}(t) \quad (10d)$$

$$\underline{V}_i \leq V_i(t) \leq \overline{V}_i \quad \forall i \in \mathcal{N} \quad \forall t \in \mathcal{T} : \mu_i^{min}(t), \mu_i^{max}(t) \quad (10e)$$

$$Q_{i,g}^{PV}(t) \leq Q_{i,max}^{PV}(t) \forall i \in \mathcal{N}^G \quad \forall t \in \mathcal{T} : \psi_{i,pv}^{max}(t) \quad (10f)$$

$$Q_{i,g}^{PV}(t) \geq Q_{i,min}^{PV}(t) \forall i \in \mathcal{N}^G \quad \forall t \in \mathcal{T} : \psi_{i,pv}^{min}(t) \quad (10g)$$

$$U_{t_k}(t) \in D_{t_k} \quad \forall k \in \mathcal{N}^T \quad \forall t \in \mathcal{T} \quad (10h)$$

$$U_{c_k}(t) \in D_{c_k} \quad \forall k \in \mathcal{N}^C \quad \forall t \in \mathcal{T} \quad (10i)$$

where  $P_{\ell}^{loss}(t)$  symbolize active power losses on a branch  $\ell$  at time  $t$ .  $\Delta \mathcal{P}_i(t)$  and  $\Delta \mathcal{Q}_i(t)$  are nodal active and reactive power equality constraints at time  $t$  which is computed as,

$$\Delta \mathcal{P}_i(t) = \mathcal{P}_i^g(t) + \mathcal{P}_{i,g}^{PV} - \mathcal{P}_i^d(t) - \sum_{j \in \Omega_i, j \neq i} \mathcal{P}_{ij}(t) \quad (11)$$

$$\Delta \mathcal{Q}_i(t) = Q_i^g(t) + Q_{i,g}^{PV} + Q_i^{sh} - Q_i^d(t) - \sum_{j \in \Omega_i, j \neq i} Q_{ij}(t) \quad (12)$$

where  $\mathcal{P}_i^g, Q_i^g$  and  $\mathcal{P}_i^d(t), Q_i^d(t)$  are nodal generated and demand active and reactive power respectively.  $\sum_{j \in \Omega_i} \mathcal{P}_{ij}(t)$  and  $\sum_{j \in \Omega_i} Q_{ij}(t)$  are the total power flow from node  $i$  where  $\Omega_i$  is a set of all nodes connected to node  $i$ .  $\mathcal{P}_{i,g}^{PV}$  and  $Q_{i,g}^{PV}$  represent PV-system generated active and reactive power respectively. The available upper and lower limits of reactive power support at time  $t$  is determined as,

$$Q_{i,max}^{PV}(t) = -Q_{i,min}^{PV}(t) = \sqrt{(\mathcal{S}_{rated}^{PV})^2 - (\mathcal{P}_{i,g}^{PV}(t))^2} \quad (13)$$

Other nomenclatures:

- $\mathcal{T}$  is a set of time segments being optimized.
- $\mathcal{L}$  is a set of all the distribution branches.
- $\mathcal{N}$  is a set of all nodes excluding a predefined slack node.
- $\mathcal{N}^T$  a set of voltage regulators and transformers with OLTC.
- $\mathcal{N}^C$  a set of all nodes with capacitor banks.
- $Q_i^{sh}$  is the shunt capacitance injected at node  $i$  by a capacitor bank (if the node has one; otherwise it equals zero).
- $V_i(t)$  is the voltage phasor of each node ( $|V_i| \angle \theta_i$ ), while  $\underline{V}_i$  and  $\overline{V}_i$  are the minimum and maximum permitted operating limits of each phasor respectively.
- $\mathcal{S}_{\ell}(t)$  is the apparent power flow on branch  $\ell$  while  $\mathcal{S}_{\ell}^{max}$  is the branch maximum thermal limit.
- $U_{t_k}(t)$  is an integer setting value of the  $k$ -th transformer's OLTC at time  $t$  and  $D_{t_k}$  is a set of the tap position numbers (it usually has 32 regulation step with a neutral step in the middle).
- $U_{c_k}(t)$  is an integer setting value of the  $k$ -th capacitor bank at time  $t$  and  $D_{c_k}$  is a set of the tap position numbers.
- $\lambda_i^P, \lambda_i^Q, \mathfrak{S}_{\ell}, \mu_i^{min}, \mu_i^{max}, \psi_{i,pv}^{max}, \psi_{i,pv}^{min}$  are dual variables associating each constraint.

### C. Model Implementation Technique (MINLP into NLP)

The aforementioned model is a mixed-integer, non-linear and non-convex optimization problem. In general there are four techniques that are commonly used to solve such a problem which are: branch and bound, branch and cut, bender decomposition and outer approximation. However, as the number of integer variables increase these methods could become computationally expensive and less robust [12], [13].

In this paper, a penalty based method which was introduced in [8], [9] and implemented in [13], [14] is adopted to solve the VVO model. It convert MINLP into a continues nonlinear problem which then can be solved directly using nonlinear local optimization solvers such as IPOPT or FMINCON.

Utilizing the formulated model in (10), the integer variables  $U_{t_k}$  and  $U_{c_k}$  are considered as bounded continuous variables while an "integerization" sinusoidal penalty function is added to the primary objective function to drive the optimization solver to achieve a feasible value for each variable. The model is updated as,

$$\min_x \sum_{t=1}^{\mathcal{T}} \sum_{\ell} P_{\ell}^{loss}(t) \cdot [\mathcal{T}_{t+1} - \mathcal{T}_t] + \gamma \Phi(U_{t_k}, U_{c_k}) \quad (14a)$$

$$\text{s.t. } (10b) - (10g)$$

$$U_{t_k}^{min} \leq U_{t_k}(t) \leq U_{t_k}^{max} \quad \forall k \in \mathcal{N}^T \quad \forall t \in \mathcal{T} \quad (14b)$$

$$U_{c_k}^{min} \leq U_{c_k}(t) \leq U_{c_k}^{max} \quad \forall k \in \mathcal{N}^C \quad \forall t \in \mathcal{T} \quad (14c)$$

with,

$$\Phi(U_{t_k}, U_{c_k}) = \sum_{k=1}^{\mathcal{N}^T} [\sin(U_{t_k} \cdot \pi)]^2 + \sum_{k=1}^{\mathcal{N}^C} [\sin(U_{c_k} \cdot \pi)]^2$$

where  $\gamma$  is a scaling parameter to control the penalty function impact weight. When the tap variables  $U_{t_k}$  and  $U_{c_k}$  obtain integer values, the penalty function would equal zero.

A loop is created around the optimization problem to push the solver into convergence by obtaining values with a certain small percentage of deviation from the feasible values of each integer variable. By gradually increasing the value of  $\gamma$ , the problem should converge into a feasible solution. However, because of the noneconvexity nature of the problem, optimal solution is not guarantee to converge into a global one [14].

### III. SENSITIVITY OF LOSS TOWARD LOADING CONDITION

The sensitivity (i.e. rate of change) of power loss toward load changes can be found using Karush-Kuhn-Tucker method (KKT). From the adopted VVO model in (10) the Lagrange function can be formulated as follows:

$$\begin{aligned} \mathcal{L}(x, U_{t_k}, U_{c_k}, \lambda_i^P, \lambda_i^Q, \mathfrak{S}_{\ell}, \mu_i^{min}, \mu_i^{max}, \psi_{i,pv}^{max}, \psi_{i,pv}^{min}) \\ = \sum_{\ell} P_{\ell}^{loss}(|V_i|, \theta_i) \\ + \lambda_i^P \left( \mathcal{P}_i^g + \mathcal{P}_{i,g}^{PV} - \mathcal{P}_i^d - \sum_{j \in \Omega_i, j \neq i} \mathcal{P}_{ij} \right) \\ + \lambda_i^Q \left( Q_i^g + Q_{i,g}^{PV} + Q_i^{sh} - Q_i^d - \sum_{j \in \Omega_i, j \neq i} Q_{ij} \right) \\ + \mathfrak{S}_{\ell} \left( \mathcal{S}_{\ell} - \mathcal{S}_{\ell}^{max} \right) + \mu_i^{min} \left( \underline{V}_i - V_i \right) \\ + \mu_i^{max} \left( V_i - \overline{V}_i \right) + \psi_{i,pv}^{max} \left( Q_{i,g}^{PV} - Q_{i,max}^{PV} \right) \end{aligned}$$

$$+ \psi_{i,pv}^{min} ( Q_{i,min}^{PV} - Q_{i,g}^{PV} ) \quad (15)$$

Where the inequality constraints dual variables  $\mathfrak{S}_\ell$ ,  $\mu_i^{min}$ ,  $\mu_i^{max}$ ,  $\psi_{i,pv}^{max}$  and  $\psi_{i,pv}^{min}$  are all greater than or equal 0.

Taking partial derivative of the Lagrange function with respect to the nodal power demand yield nodal active and reactive locational sensitivity of loss toward nodal loading condition:

$$\frac{\partial \mathcal{L}}{\partial P_i^d} = \lambda_i^P \quad (16)$$

$$\frac{\partial \mathcal{L}}{\partial Q_i^d} = \lambda_i^Q \quad (17)$$

Power losses across distribution lines are the result of the flowing current interacting with the line impedance producing heat, voltage drop and decreased power transfer capacity on that line. As the current magnitude rise, power losses increase consequently ( $I^2 \times R$ ). Thus, the dual variables ( $\lambda_i^P$  and  $\lambda_i^Q$ ) provide efficacious indications to predict nodal response toward load changes or active/reactive power compensation.

This present a way to price DER power purchase agreements based on the location and area loading condition. Owners in condensed areas with high value of sensitivity of loss toward load increase ( $\lambda_i^P$  or  $\lambda_i^Q$ ) ought to be offered higher financial incentives to encourage them to participate in supplying local demand and reduce power transmission losses.

#### IV. CASE STUDIES AND RESULTS INTERPRETATION

The mixed-integer nonlinear VVO model formulated in (10) is solved through the approach demonstrated in section (II-C) using local nonlinear optimization solver FMINCON which is part of MATLAB optimization toolbox. A modified IEEE-69 distribution system shown in Fig. 2 with a base voltage of 12.6kV and 10MVA base apparent power is adopted to simulate a typical mid-size system. Network branch data are obtained from [15], [16]. A distribution transformer with an OLTC is considered between nodes 1 and 2 with 32 voltage regulation steps ( $\pm 10\%$  of input voltage).

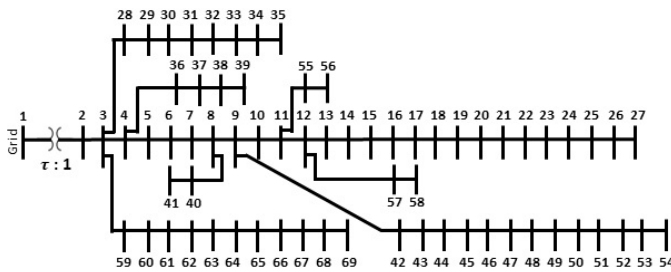


Fig. 2: Modified IEEE-69 Node Distribution System

Nodes are assumed to have various power demand charts during a 24 hour period with constant power factors. Charts are showing in Fig. 3 while table I lists each node's specific chart.

Nodal voltage maximum and minimum limits are 1.05 and 0.95 respectively. Moreover, all branches are assumed to have

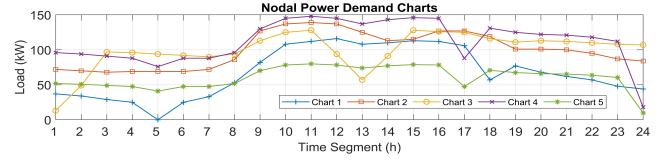


Fig. 3: Nodal Power Demand Charts  
Table I. List of Nodal Loading Charts

	Node Number
Chart 1	2 9 28 29 33 34 36 40 41 45 46 57-60 62-64 66 68 69
Chart 2	5 31 42-44 47 48 50 51 53-56 67
Chart 3	6-8 10-13 15-17 20 21 23 26 27
Chart 4	30 37-39 61
Chart 5	22 25

a thermal limit of 10 MVA. Lastly, the OLTC tap discrete variable  $\tau_1$  parameters are:  $\tau_1^{min} = 0.9$ ,  $U_{t_1} = \{0, 1, 2, \dots, 32\}$  and  $\delta_1^t = 5/8\%$ .

Two case studies are conducted to demonstrate the concept thoroughly. Computation results were validated using MATPOWER package [17] to ensure strict accuracy.

#### A. Case One: A Broad View

1) *System in Original Status*: Fig. 4 depicts the system original active and reactive locational sensitivity of loss toward load changes during a 24 hour period. Elevated  $\lambda_i^P$  and  $\lambda_i^Q$  ratios reflect rising loading levels in a direct correlation. Nodal voltage profiles during the 24-hour period are shown in Fig. 5. Although all nodes are within permissible limits, some nodes are at risk of voltage drop with additional load.

A closer look at an average loading level at time segment 14 is presented in Fig. 6. It depicts a parallel comparison of locational  $\lambda_i^P$  and  $\lambda_i^Q$ , nodal voltage profile, active and reactive power flow and power losses across branches. Power loss depends upon the line impedance and the flowing current magnitudes. Thus, some branches have higher loss ratio than other although they has less  $\lambda_i^P$  and  $\lambda_i^Q$  values.

Since the distribution feeder from node 1 to 27 is the main line where remaining nodes branch out of it. Loading on lateral lines affect the node of branching on the main line. Thus, to

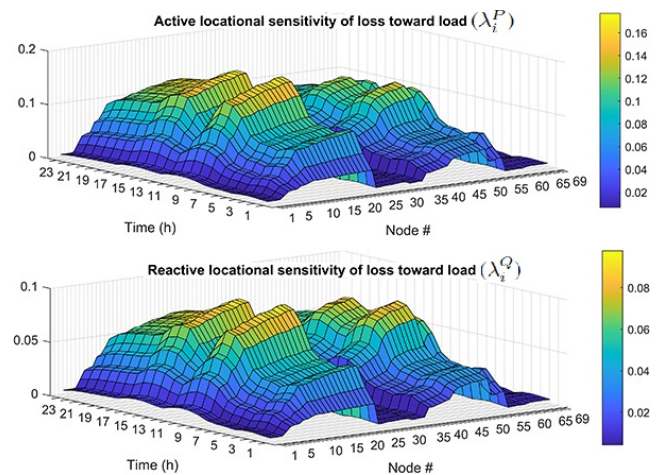


Fig. 4: Loss Locational Sensitivity toward Loading Condition

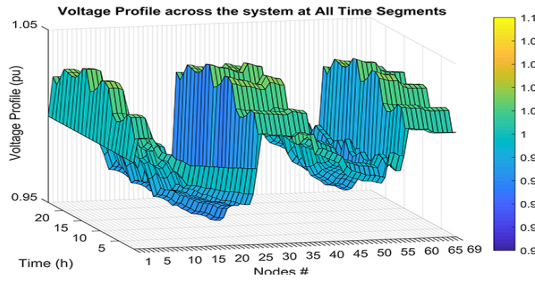


Fig. 5: Nodal Voltage Profile

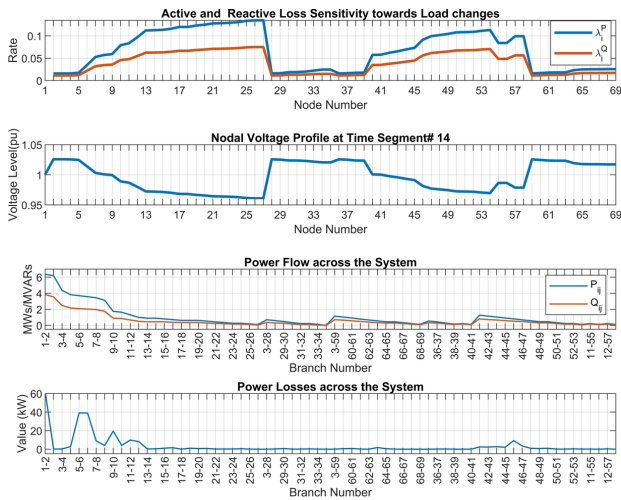


Fig. 6: Comprehensive Analysis of time segment 14

provide a clear charts and reduce the number of figures, it is adequate to present impact upon the main line exclusively.

2) *Implementing Active and Reactive Power Compensation:* An elaborated examination of  $\lambda_i^P$  and  $\lambda_i^Q$  charts in Fig. 6 indicate to a necessity at various parts of the network for active and reactive power compensation. Nodes with elevated  $\lambda_i^P$  and  $\lambda_i^Q$  ratios require power compensation to partially supply local demand and reduce losses. Therefore, two scenarios are performed to show the effect of power compensation on the system and examine nodal loss sensitivity variation toward loading condition.

Scenario 1: in light of Fig. 6, three capacitor banks with a total capacity of 900 kVARs per bank are installed at nodes 8, 13 and 45 for a capacitive power compensation. Each bank contains three internal capacitors with a capacity of 300kVARs each. The parameters of all capacitor banks tap discrete variable  $b_k^{sh}$  are:  $b_k^{\min} = 0$ ,  $U_{ck} = \{0, 1, 2, 3\}$  and  $\delta_k^c = 3\%$ .

Scenario 2: in addition to the connected capacitor banks, several nodes are assumed to have PV-systems with different capacity as shown in table II where  $P_{\text{rated}}^{\text{PV}}$  refer to the PV-panels rated maximum capacity while  $S_{\text{rated}}^{\text{PV}}$  represent the inverter maximum operating limit. Values are assumed for experimental aspects and not based on industrial standards. All PV-systems are allowed to supply and consume reactive power based on the inverter capacity.

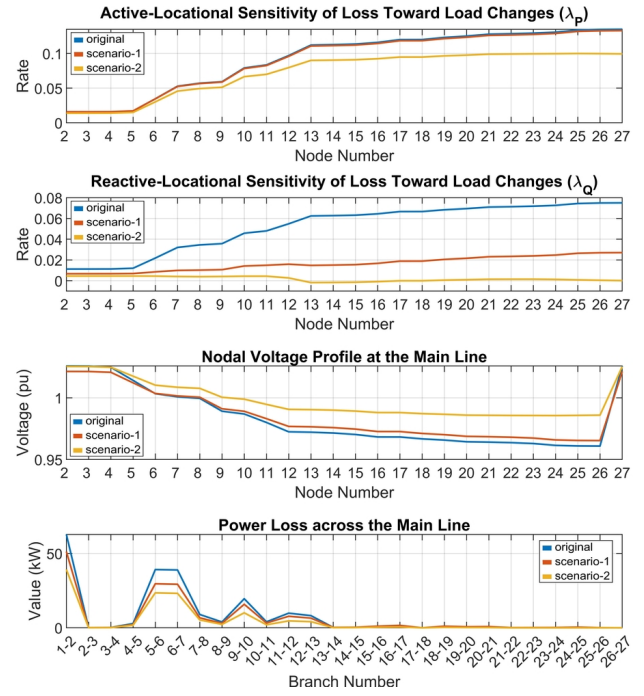


Fig. 7: Case Study 1: Three Different Scenarios.

Fig. 7 reveals a system-wide glance showing a comparison of the original status with the proposed two scenarios. It can be observed that in the original status (blue line)  $\lambda_i^P$  and  $\lambda_i^Q$  values are raising after node 5 and continue to rise due to the loading conditions and high line impedance. The reactive-locational sensitivity of loss toward load  $\lambda_i^Q$  is utilized to identify optimal placement of capacitor banks at nodes 8, 13 and 45 which appeared clearly in the first compensation scenario (red line). Implementing these capacitors reduced line loss and improved voltage profile. Furthermore, active-locational sensitivity of loss toward load  $\lambda_i^P$  is utilized to identify optimal placement for active power compensation which yield a superior voltage profile and reduced loss significantly in the second scenario (yellow line).

Note that in the second scenario, nodes 13 and 14 has a negative  $\lambda_i^Q$  which indicate to an overcompensation situation due to excessive VAR supply by DER inverters. Such a power security issue motivates distribution network operators (DNOs) and power legislators to impose various standards such as (IEEE Std. 1547-2003) to oblige DER owners to operate with a unity or a specific power factor to prevent uncontrolled or undesired VAR supply. Furthermore, loading levels during the three performed scenarios are fixed. However, in case inductive loads at nodes 13 and 14 increase during the second scenario, power losses will exceptionally be reduced.

The optimization optimal results during the three performed cases are: in the original status;  $\tau_1 = 0.9499$  ( $TAP\#9$ ), in scenario-1;  $\tau_1 = 0.9625$  ( $TAP\#11$ ),  $b_1^{sh} = 0.0602$ ,  $b_2^{sh} = 0.0603$ ,  $b_3^{sh} = 0.0602$ , and finally in scenario-2;  $\tau_1 = 0.9623$  ( $TAP\#11$ ),  $b_1^{sh} = 0.0603$ ,  $b_2^{sh} = 0.0600$ ,  $b_3^{sh} = 0.0603$  while PV-systems optimal settings are listed in Fig. 8.

Table II. Distributed PV-Systems Data

Node #	$P_{PV}^{rated}$	$S_{PV}^{rated}$	Node #	$P_{PV}^{rated}$	$S_{PV}^{rated}$
10	15	18	30	15	18
12	45	54	35	250	300
18	15	60	54	45	54
20	15	18	62	15	18
26	15	18	67	15	18
27	250	300	69	45	54

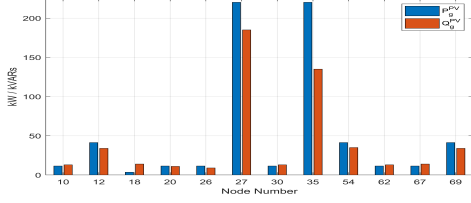


Fig. 8: Optimal DER Power Dispatch

### B. Case Two: Close Examination

A second case study is carried out to inspect the influence of a particular node load change on surrounding nodes levels of  $\lambda_i^P$  and  $\lambda_i^Q$  and power factors during time segment 14.

A particular part of the system from node 36 to 39 is monitored closely while loading level on node 38 varies in three different scenarios. Fig. 9 depicts a comparison of the three performed tests.

The first scenario (blue line) represent the original status of the system at time segment 14. In the second scenario, node 38 active power demand is increased 300%. For a third scenario, its reactive power demand is increased 300%. It can be observed that increasing active power demand at node 38 in the second scenario (red line) raised  $\lambda_i^P$  value which illustrate that augmenting more active load will produce higher power losses. It slightly reduced  $\lambda_i^Q$  value because the ratio of active to reactive power demand is increased which is shown clearly as a power factor improvement. However, raising active power demand increased branch losses. As for the third scenario (yellow line), increasing reactive power demand at node 38 increased  $\lambda_i^Q$  value which state that augmenting additional inductive load will raise power loss. As expected, it decreased nodal power factors due to the increase of inductive load.

### V. CONCLUSION

This paper review the potential utilization of the dual variables associating power equality constraints in VVO models as tools to predict loss sensitivity toward load changes. Results can be used to determine optimal placement of active and reactive power compensation equipment. In addition, it can be utilized to price DER generated power based upon location. A detailed formulation of a mixed-integer nonlinear VVO models is illustrated and a solving technique is presented and validated.

### REFERENCES

[1] M. Hong, "An approximate method for loss sensitivity calculation in unbalanced distribution systems," *IEEE Transactions on Power Systems*, vol. 29, no. 3, pp. 1435–1436, May 2014.  
 [2] X. Cheng, T. Wang, and H. Zheng, "Reactive power optimization of genetic algorithm based on sensitivity analysis," *DEStech Transactions on Environment, Energy and Earth Sciences*, no. appecc, 2018.

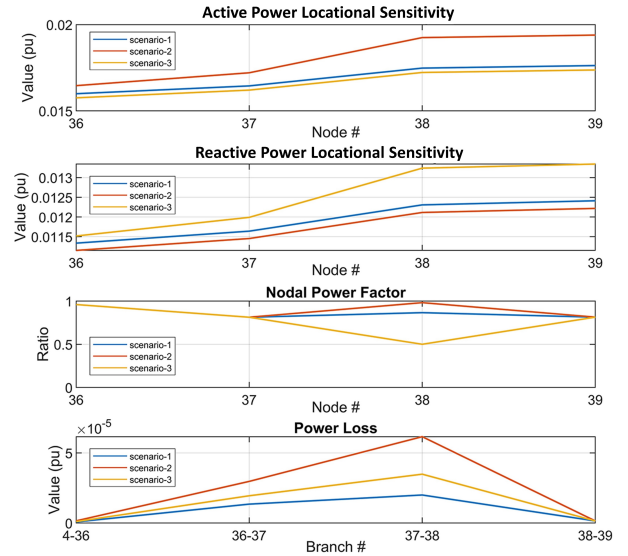


Fig. 9: A Comparison of Three Different scenarios.

[3] D. K. Khatod, V. Pant, and J. Sharma, "A novel approach for sensitivity calculations in the radial distribution system," *IEEE transactions on Power Delivery*, vol. 21, no. 4, pp. 2048–2057, 2006.  
 [4] J. E. Candelo and H. Hernández, "Location and size of distributed generation to reduce power losses using a bat-inspired algorithm," in *VII Simposio Internacional sobre Calidad de la Energía Eléctrica*, 2013.  
 [5] M. Santiago-Luna and J. R. Cedeno-maldonado, "Optimal placement of facts controllers in power systems via evolution strategies," pp. 1–6, Aug 2006.  
 [6] L. Bai, J. Wang, C. Wang, C. Chen, and F. Li, "Distribution locational marginal pricing (dlmp) for congestion management and voltage support," *IEEE Transactions on Power Systems*, 2017.  
 [7] Z. Liu, Q. Wu, S. Oren, S. Huang, R. Li, and L. Cheng, "Distribution locational marginal pricing for optimal electric vehicle charging through chance constrained mixed-integer programming," *IEEE Transactions on Smart Grid*, 2016.  
 [8] J.-F. Fu, R. G. Fenton, and W. L. Cleghorn, "A mixed integer-discrete-continuous programming method and its application to engineering design optimization," *Engineering Optimization*, vol. 17, no. 4, pp. 263–280, 1991.  
 [9] E. Davydov and I. K. Sigal, "Application of the penalty function method in integer programming problems," *Engineering Cybernetics*, vol. 10, no. 1, pp. 21–24, 1972.  
 [10] A. R. Bergen and V. Vittal, *Power systems analysis*. Prentice Hall, 2000.  
 [11] E. Liu and J. Bebic, "Distribution system voltage performance analysis for high-penetration photovoltaics."  
 [12] P. Belotti, C. Kirches, S. Leyffer, J. Linderoth, J. Luedtke, and A. Mahajan, "Mixed-integer nonlinear optimization," *Acta Numerica*, vol. 22, pp. 1–131, 2013.  
 [13] F. M. de Vasconcelos, G. R. da Costa, and G. G. Lage, "An nlp penalty-based strategy for handling discrete controls for volt/var optimization in distribution systems," in *Power & Energy Society General Meeting, 2015 IEEE*. IEEE, 2015, pp. 1–5.  
 [14] E. M. Soler, E. N. Asada, and G. R. Da Costa, "Penalty-based nonlinear solver for optimal reactive power dispatch with discrete controls," *IEEE transactions on power systems*, vol. 28, no. 3, pp. 2174–2182, 2013.  
 [15] M. E. Baran and F. F. Wu, "Optimal capacitor placement on radial distribution systems," *IEEE Transactions on power Delivery*, vol. 4, no. 1, pp. 725–734, 1989.  
 [16] A. Mohapatra, P. R. Bijwe, and B. K. Panigrahi, "An efficient hybrid approach for volt/var control in distribution systems," *IEEE Transactions on Power Delivery*, vol. 29, no. 4, pp. 1780–1788, 2014.  
 [17] R. D. Zimmerman, C. E. Murillo-Sánchez, R. J. Thomas *et al.*, "Matpower: Steady-state operations, planning, and analysis tools for power systems research and education," *IEEE Transactions on power systems*, vol. 26, no. 1, pp. 12–19, 2011.